Advances in compact proton spectrometers for inertial-confinement fusion and plasma nuclear science[a)]

F. H. Seguin,[1,b)] N. Sinenian,[1] M. Rosenberg,[1] A. Zylstra,[1] M. J.-E. Manuel,[1] H. Sio,[1] C. Waugh,[1] H. G. Rinderknecht,[1] M. Gatu Johnson,[1] J. Frenje,[1] C. K. Li,[1] R. Petrasso,[1] T. C. Sangster,[2] and S. Roberts[2]
[1]*Plasma Science and Fusion Center, Massachusetts Institute of Technology, Cambridge, Massachusetts 02139, USA*
[2]*Laboratory for Laser Energetics, University of Rochester, Rochester, New York 14623, USA*

(Presented 8 May 2012; received 7 May 2012; accepted 7 June 2012; published online 24 July 2012)

Compact wedge-range-filter proton spectrometers cover proton energies ~3–20 MeV. They have been used at the OMEGA laser facility for more than a decade for measuring spectra of primary D^3He protons in D^3He implosions, secondary D^3He protons in DD implosions, and ablator protons in DT implosions; they are now being used also at the National Ignition Facility. The spectra are used to determine proton yields, shell areal density at shock-bang time and compression-bang time, fuel areal density, and implosion symmetry. There have been changes in fabrication and in analysis algorithms, resulting in a wider energy range, better accuracy and precision, and better robustness for survivability with indirect-drive inertial-confinement-fusion experiments. © *2012 American Institute of Physics*. [http://dx.doi.org/10.1063/1.4732065]

I. INTRODUCTION

Charged-particle spectrometry has long been known to be important for diagnosing inertial-confinement-fusion (ICF) plasmas,[1–5] but one of the first large-scale applications began with the installation of two magnet-based charged-particle spectrometers (CPSs)[6–8] at the OMEGA laser facility.[9] They can each measure the spectra of several particle species (e.g., p, D, T, ^{3}He, ^{4}He) simultaneously, using a 7.6-kG permanent magnet for energy discrimination and CR-39 nuclear track detectors[8,10,11] for particle detection. Of particular importance are (1) knock-on D and T from room-temperature and cryogenic DT-filled targets, for study of fuel areal density (ρR) (Refs. 12 and 13); (2) knock-on protons from DT-filled CH targets for study of shell ρR (Ref. 12); (3) D^3He protons from D^3He-filled targets for study of shell ρR;[14] and (4) energetic ions from the laser-ablated shells of OMEGA ICF capsules.[7,15] The two CPSs view an implosion from different directions, enabling rudimentary symmetry measurements.

Much simpler instruments, known as wedge-range-filter (WRF) spectrometers and described in Sec. II, were developed specifically for the study of protons.[8,16,17] They can measure proton spectra at much lower yields than the CPSs (by two orders of magnitude), and their small size (~5 cm) means that many can be deployed simultaneously at different angles for symmetry studies. First-generation WRF spectrometers were deployed in 2001 and followed later by improved versions described in Sec. III. Their sensitivity and utility for measuring spectra of primary D^3He protons, knock-on protons, and secondary D^3He protons[16] have led to WRF spectrometers becoming standard instruments for the study of shell and fuel ρR in direct drive,[16,18–22] indirect drive,[23,24] and shock ignition[25] implosions. They have been used for studies of ρR and ρR asymmetry in implosions of capsules filled with D^3He gas,[17,24,26–28] D_2 gas,[16,23,24] and DT gas.[29] A highlight was verification of the milestone achievement of ρRs of 200 mg/cm^2 at OMEGA (Refs. 18–20) in 2008. The high WRF sensitivity has made possible the study of mix[30] by imploding a CH shell with a CD sublayer, filled with pure ^{3}He gas, and looking for D^3He protons that can only be produced if there is fuel-shell mix.

Since 2009, WRFs have also been in regular use with indirect-drive implosions at the National Ignition Facility (NIF),[31] where measurements have been made simultaneously from the polar direction (through the laser entrance hole) and from the equatorial direction (this spectrum must be corrected for slowing in the hohlraum wall). Such pairs of measurements provide a measure of implosion symmetry.[32]

In the case of primary D^3He protons, spectra have separate parts produced at shock-bang time and at compression-bang time (Fig. 2(a)). This means that ρR at the two times can be determined separately. That is particularly useful when a time history of proton production is also measured, either by the proton temporal diagnostic[27] at OMEGA or by the particle time-of-flight diagnostic[33] at OMEGA or the NIF, so that details of implosion dynamics can be compared in detail with simulations.

At OMEGA, WRFs have recently assumed new importance in measurements of ^{3}He-^{3}He protons for study of nucleosynthesis reactions[34] in the new field of plasma nuclear science.[35,36]

[a)]Contributed paper, published as part of the Proceedings of the 19th Topical Conference on High-Temperature Plasma Diagnostics, Monterey, California, May 2012.
[b)]Author to whom correspondence should be addressed. Electronic mail: seguin@mit.edu.

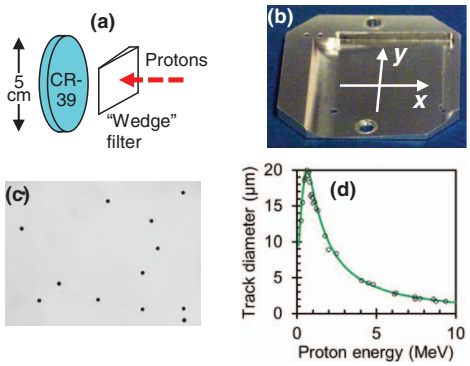

FIG. 1. The active part of a WRF spectrometer (a) consists of a CR-39 nuclear track detector behind a "wedge" filter with thickness increasing in the x direction (b). Protons that pass through the filter leave trails of molecular damage in the CR-39 which, when etched, appear under a microscope as dark circular tracks (c) whose diameters are related to the energies of the protons after passing through the WRF through the function $D(E)$ (d). Combining the track information with the WRF filter thickness and $D(E)$ produces the spectrum of the protons that were incident on the WRF (see Fig. 2).

II. WRF PROTON SPECTROMETERS

Figures 1(a) and 1(b) illustrate the components of a WRF spectrometer. Protons pass through a wedge-shaped ranging filter, whose thickness T varies in the x direction, before striking a CR-39 nuclear track detector. After being etched for a few hours in 6-normal NaOH at 80 °C, the surface of the CR-39 has circular tracks where each proton entered (Fig. 1(c)). The diameter D and position (x, y) of every track are recorded by an automated scanning microscope. The diameter is used to determine the energy E of the corresponding proton when it entered the CR-39, through a relationship $D(E)$ such as that shown in Fig. 1(d), and the energy of the same proton before it passed through the filter is then determined through use of the thickness T of the filter at position (x,y). Once this process is followed for all tracks within a specified diameter range (typically 7–16 μm), the distribution of measured proton energies is combined with the area of the region in which each energy can be detected and the known geometric parameters of the detector to form a spectrum of the protons that were incident on the front of the spectrometer (examples are shown in Fig. 2).

The WRF thickness T is nominally a function only of x, but fabrication issues generally result in a small variation with y that must be determined. $T(x,y)$ is inferred from data collected by exposing a WRF to protons of known energies from a linear accelerator.[37] D^3He protons from fusion reactions in the accelerator target are passed through filters overlaid on the WRF to produce data simultaneously at 2 or 3 discrete energies that are, themselves, determined to an accuracy of ~0.05 MeV with a separate calibration process.

The accuracy of a spectrum depends on uncertainties in both $T(x,y)$ and $D(E)$. Originally, $D(E)$ was measured with accelerator-generated protons[8] and was found to be repeatable (Fig. 1(d)). Recent accelerator-based measurements[38] and WRF data have indicated sample-to-sample variations in $D(E)$ for current CR-39, so new methods have been developed to determine $D(E)$ self-consistently from WRF data during analysis (see Sec. III).

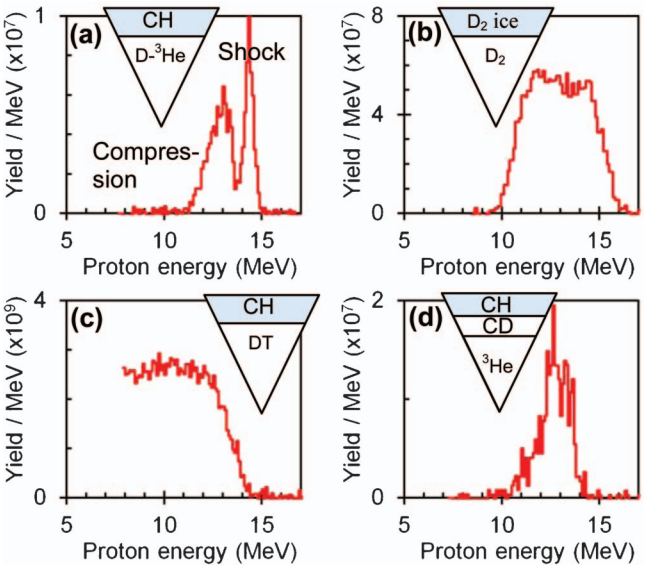

FIG. 2. WRF proton spectra from four types of implosions on OMEGA, with shell and gas fill compositions shown. Shot numbers are: 25 688, 28 900, 23 445, and 22 063 (a)–(d).

III. MODIFICATIONS AND IMPROVEMENTS

A first-generation aluminum WRF from 2001 is shown in Fig. 1(b). It can be used as close to the OMEGA target chamber center (TCC) as 10.5 cm without interfering with laser beams, and it works at proton yields as low as a few $\times 10^5$. With minimum and maximum thicknesses of 400 and 1800 μm, it covers the proton energy range 8–18 MeV.

The first variation on this design was a miniature aluminum WRF (Fig. 3(a)) made in 2002 for use as close to TCC as 4 cm for certain experiments with very low yields. Its energy range is 7–15 MeV, and it was used to make the first ρR symmetry measurements with indirect drive implosions at OMEGA.[23]

A different design was developed in 2004, when low-adiabat experiments with D_2-filled targets and thick CH shells at OMEGA began to result in areal densities high enough to require proton spectral measurements below 8 MeV. It was anticipated that areal densities of cryogenic D_2 targets would soon approach 200 mg/cm^2 and generate secondary protons at energies as low as 3 MeV. Measuring proton spectra at energies below 8 MeV with an aluminum WRF requires that the thin part of the filter be substantially thinner than the original 400 μm, but fabrication experiments showed that it was difficult to achieve this with sufficient accuracy. Instead, new WRFs were made of the ceramic material zirconia in

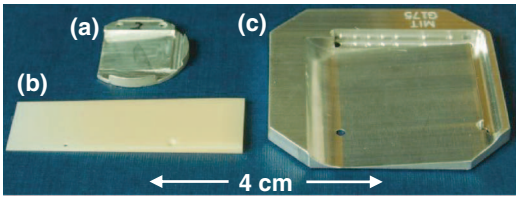

FIG. 3. Miniature aluminum WRF from 2002 (a), broad band zirconia WRF from 2004 (b), and broad band aluminum WRF from 2010 (c). Each one has at least two holes used for imprinting position fiducials on CR-39.

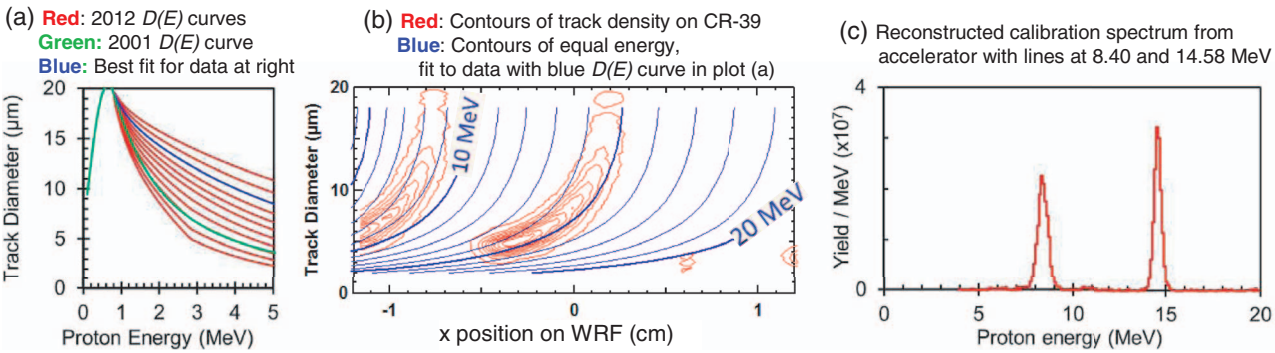

FIG. 4. The range of *D(E)* behavior observed in recent CR-39 (a), and an example of the process of extracting a proton spectrum (c) from WRF proton track data (b). (The 8.4-MeV line is wider because of straggling in the filter used to range it down from 14.58 MeV.)

a very simple design with thickness varying linearly from about 40 μm to 1600 μm (Fig. 3(b)). With a 25-μm-thick Al blast filter, the low-energy measurement limit is 3.5–4 MeV. This was sufficient to verify the milestone achievement of 200 mg/cm^2 in 2008, as described in Sec. I.

The zirconia WRFs are brittle and susceptible to cracking and chipping from handling and/or exposure to difficult conditions in the target chamber (particularly hohlraum debris). Because of this, a new technique was developed in 2010 for fabrication of an aluminum WRF that can be made quite thin ($\sim$130 μm) while still maintaining surface machining tolerances of a few microns (Fig. 3(c)). This new design provides a low-energy limit close to that of the zirconia WRFs while being far more robust and resistant to damage.

There have also been important improvements in analysis algorithms to compensate for the fact that recent CR-39 shows large sample-to-sample variations in *D(E),* as illustrated in Fig. 4(a). There are ways to extract the effective *D(E)* from a WRF scan file, since analysis of each small interval in track diameter must result in the same inferred proton spectrum. This is illustrated in Fig. 4 for an accelerator exposure of a WRF with two discrete proton energies.

The net result of these changes and improvements is shown in Table I. The energy precision is determined empirically by exposing a single WRF many times to protons of known energies using different CR-39 samples, and seeing how much scatter there is in the inferred energies. This includes any consequences of variability in the CR-39 samples, variability in the etching of the CR-39, and variability in the scanning process due to use of different microscopes by different people, and the result is 0.03 MeV (standard deviation). The absolute energy uncertainty of 0.06 MeV is due to the precision uncertainty combined with the uncertainty in the accelerator calibration energies (0.05 MeV).

TABLE I. Comparison of WRF performance parameters for 15-MeV protons achievable in 2001 and 2012 (not including statistical uncertainties).

	2001	2012
Energy range	8–18 MeV	3.5–20 MeV
Absolute energy uncertainty	0.15 MeV[a]	0.06 MeV
Energy precision	0.15 MeV[a]	0.03 MeV
Yield uncertainty	15%[a]	5%

[a]These values could only be achieved with piece-to-piece consistency in CR-39, which is not available in 2012.

ACKNOWLEDGMENTS

The work described here was supported in part by the (U.S.) Department of Energy (DOE) (Grant No. DE FG03-03SF22691) and the Laboratory for Laser Energetics (Grant No. 412160-001G).

[1]D. C. Slater and F. J. Mayer, Laser Interact. Relat. Plasma Phenom. **4B**, 603 (1997).
[2]S. Skupsky and S. Kacenjar, J. Appl. Phys. **52**, 2608 (1981).
[3]H. Azechi *et al.*, Appl. Phys. Lett. **49**, 555 (1986).
[4]Y. Kitagawa *et al.*, Phys. Rev. Lett. **75**, 3130 (1995).
[5]M. D. Cable *et al.*, Plasma Phys. Rep. **24**, 110 (1998).
[6]D. G. Hicks *et al.*, Rev. Sci. Instrum. **68**, 589 (1997).
[7]D. G. Hicks, "Charged-particle spectroscopy: a new window on inertial confinement fusion," Ph.D. dissertation (Massachusetts Institute of Technology, 1999).
[8]F. H. Seguin *et al.*, Rev. Sci. Instrum. **74**, 975 (2003).
[9]T. R. Boehly *et al.*, Opt. Commun. **133**, 495 (1997).
[10]R. L. Fleischer, P. B. Price, and R. M. Walker, *Nuclear Tracks in Solids, Principles and Applications* (University of California, 1975).
[11]A. P. Fews, M. J. Lamb, and M. Savage, Opt. Commun. **98**, 159 (1993).
[12]C. K. Li *et al.*, Phys. Plasmas **8**, 4902 (2001).
[13]J. A. Frenje *et al.*, Phys. Plasmas **16**, 042704 (2009).
[14]C. K. Li *et al.*, Phys. Plasmas **7**, 2578 (2000).
[15]D. G. Hicks Phys. Plasmas **8**, 606 (2001).
[16]F. H. Seguin *et al.*, Phys. Plasmas **9**, 2725 (2002).
[17]F. H. Seguin *et al.*, Phys. Plasmas **9**, 3558 (2002).
[18]T. C. Sangster *et al.*, Phys. Rev. Lett. **100**, 185006 (2008).
[19]V. N. Goncharov *et al.*, Phys. Plasmas **15**, 056310 (2008).
[20]R. L. McCrory *et al.*, Phys. Plasmas **15**, 055503 (2008).
[21]F. J. Marshall *et al.*, Phys. Rev. Lett. **102**, 185004 (2009).
[22]P. B. Radha *et al.*, Phys. Plasmas **18**, 012705 (2011).
[23]C. K. Li *et al.*, Bull. Am. Phys. Soc. **48**, 57 (2003).
[24]F. Philippe *et al.*, Phys. Rev. Lett. **104**, 035004 (2010).
[25]W. Theobald *et al.*, Plasma Phys. Controlled Fusion **5**, 124052 (2009).
[26]C. K. Li *et al.*, Phys. Rev. Lett. **92**, 205001 (2004).
[27]J. A. Frenje *et al.*, Phys. Plasmas **11**, 2798 (2004).
[28]C. K. Li *et al.*, Phys. Plasmas **10**, 1919 (2003).
[29]J. A. Frenje *et al.*, Phys. Plasmas **9**, 4719 (2002).
[30]C. K. Li *et al.*, Phys. Rev. Lett. **89**, 165002 (2002).
[31]G. H. Miller, E. I. Moses, and C. R. Wuest, Nucl. Fusion **44**, S228 (2004).
[32]A. Zylstra *et al.*, Rev. Sci. Instrum. **83**, 10D901 (2012).
[33]H. Rinderknecht *et al.*, Rev. Sci. Instrum. **83**, 10D902 (2012).
[34]J. A. Frenje *et al.*, private communication (2012).
[35]J. A. Frenje *et al.*, Phys. Rev. Lett. **107**, 122502 (2011).
[36]D. T. Casey *et al.*, Phys. Rev. Lett. **108**, 075002 (2012).
[37]N. Sinenian *et al.*, Rev. Sci. Instrum. **83**, 043502 (2012).
[38]M. J.-E. Manuel *et al.*, Rev. Sci. Instrum. **82**, 095110 (2011).